

# Robustness portraits of diverse biological networks conserved despite order-of-magnitude parameter uncertainty

Anthony R. Soltis and Jeffrey J. Saucerman\*

Department of Biomedical Engineering, University of Virginia, Box 800759, Charlottesville, VA 22908, USA

Associate Editor: Trey Ideker

## ABSTRACT

**Motivation:** Biological networks are robust to a wide variety of internal and external perturbations, yet fragile or sensitive to a small minority of perturbations. Due to this rare sensitivity of networks to certain perturbations, it is unclear how precisely biochemical parameters must be experimentally measured in order to accurately predict network function.

**Results:** Here, we examined a model of cardiac  $\beta$ -adrenergic signaling and found that its robustness portrait, a global measure of steady-state network function, was well conserved even when all parameters were rounded to their nearest 1–2 orders of magnitude. In contrast,  $\beta$ -adrenergic network kinetics were more sensitive to parameter precision. This analysis was then extended to 10 additional networks, including *Escherichia coli* chemotaxis, stem cell differentiation and cytokine signaling, of which nine exhibited conserved robustness portraits despite the order-of-magnitude approximation of their biochemical parameters. Thus, both fragile and robust aspects of diverse biological networks are largely shaped by network topology and can be predicted despite order-of-magnitude uncertainty in biochemical parameters. These findings suggest an iterative strategy where order-of-magnitude models are used to prioritize experiments toward the fragile network elements that require precise measurements, efficiently driving model revision.

**Contact:** jsaucerman@virginia.edu

**Supplementary information:** Supplementary data are available at *Bioinformatics* online.

Received on May 11, 2011; revised on August 12, 2011; accepted on August 25, 2011

## 1 INTRODUCTION

Robustness is a key emergent property of many biological systems (Kitano, 2004; Stelling *et al.*, 2004). Systems are considered robust if they are able to retain core functionality in the face of external (e.g. temperature, ligand concentration) and internal (e.g. gene or protein expression) perturbations. Robustness despite variations in biochemical parameters has been observed in a number of computational and experimental studies, including bacterial chemotaxis (Alon *et al.*, 1999; Barkai and Leibler, 1997; Kollmann *et al.*, 2005), segment polarity in insect development (Meir *et al.*, 2002; von Dassow *et al.*, 2000), NF $\kappa$ B oscillations (Paszek *et al.*, 2010; Tay *et al.*, 2010) and osmoregulation (Krantz *et al.*, 2009; Muzzey *et al.*, 2009; Shinar and Feinberg, 2010). Network robustness leads to the hypothesis that proper network function

does not require fine-tuning of biochemical parameters (Barkai and Leibler, 1997).

However, many of these studies have also shown that the same network can be highly sensitive to certain perturbations, leading to the qualification that complex networks are ‘robust, yet fragile’ (Cséte and Doyle, 2002). A fundamental challenge presented by this alternate view is that, without having measured all biochemical parameters with high precision *a priori*, it is uncertain whether one could accurately predict to which perturbations a network is ‘fragile’ or ‘robust’.

In this study we asked, ‘What is the quantitative precision of biochemical parameters required to accurately predict the ‘robust yet fragile’ nature of a biological network?’ Starting with a well-validated model of cardiac  $\beta$ -adrenergic signaling (Saucerman *et al.*, 2004), we systematically characterized this network’s steady-state functional relationships, or robustness portrait, with both the original, fine-tuned model and a model in which each parameter was rounded to its nearest order of magnitude. The order-of-magnitude parameter approximation introduced here is analogous to techniques widely used in physics and engineering. Robustness portraits of the original and approximate models were well correlated, even when parameters were approximated to their nearest two orders of magnitude. Order-of-magnitude approximate models also outperformed randomized models of equivalent parameter variance. We then applied the order-of-magnitude analysis to 10 additional biological networks and found that most networks were similarly insensitive to order-of-magnitude parameter estimates. This indicates that quantitative functional relationships are largely shaped by network topology. The ability to predict the ‘robust yet fragile’ nature of biological networks despite order-of-magnitude parameter uncertainty suggests a strategy where order-of-magnitude models are used to identify the experiments that reveal the most fragile, information-rich aspects of a biological network, efficiently guiding model refinement.

## 2 METHODS

### 2.1 Computational models

All model simulations were performed in MATLAB (Mathworks, Natick, MA, USA) using the stiff ordinary differential equation (ODE) solver ode15s. We implemented our computational model of cardiac  $\beta$ -adrenergic signaling (Saucerman *et al.*, 2004), excluding connected models of excitation contraction coupling. In addition, we obtained 10 computational models from either the BioModels database (Le Novère *et al.*, 2006) or the database of quantitative cellular signaling (DOQCS) (Sivakumaran *et al.*, 2003). Models from the BioModels database were obtained in SBML format and converted to MATLAB script using the Systems Biology Workbench’s BioModels

\*To whom correspondence should be addressed.

Importer (Sauro *et al.*, 2003). The model from DOQCS was implemented directly as a MATLAB script.

## 2.2 Sensitivity analysis

Sensitivity matrices for each model were generated by comparing the steady-state values of all state variables (species) from the unperturbed model against models in which individual model parameters were altered by a set percentage. Initial conditions from the original model were retained for perturbed models. Individual elements of sensitivity matrices were computed according to the equation  $S_{ij} = (\Delta Y_i / \Delta P_j) (P_{o,j} / Y_{o,i})$ , where  $S_{ij}$  is an individual, steady-state sensitivity coefficient for species '*i*' when parameter '*j*' is perturbed.  $\Delta Y_i$  is the steady-state change in species '*i*' when parameter '*j*' is altered by  $\Delta P_j$ . These sensitivities are normalized to the original steady-state value of output '*i*' ( $Y_{o,i}$ ) and parameter '*j*' ( $P_{o,j}$ ). For example, if a 5% increase in the value of parameter #2 causes a 4% decrease in the steady-state level of variable #3, the corresponding sensitivity coefficient  $S_{32}$  is  $-0.8$ . Each column in the sensitivity matrix represents a single simulation in which a single parameter value was adjusted (typically by 5%) and the resulting steady-state changes in all model outputs were computed. Thus, these matrices show a total of  $n_i \times n_j$  predictions from  $n_j$  numerical experiments.

## 2.3 Order of magnitude parameter approximations, parameter randomization, correlation analysis

Order-of-magnitude approximations were implemented according to the function:

$$\text{OOMPA}(p_o, n_{\text{OOM}}) = 10^{n_{\text{OOM}} \text{round}(\log_{10}(p_o)/n_{\text{OOM}})} \quad (1)$$

where the parameter  $n_{\text{OOM}}$  describes the roughness of each approximation and is not restricted to integer values. For example,  $n_{\text{OOM}} = 0.5$  will round parameters to their nearest half order-of-magnitude approximation,  $n_{\text{OOM}} = 1$  rounds parameters to their nearest one order of magnitude, etc.  $p_o$  denotes the vector of original parameter values. The function  $\text{round}(x)$  rounds its argument to the nearest integer (fractions with 0.5 are rounded up). A visualization of this procedure is provided in Figure 1C. For example, based on Equation (1) and Figure 1C, we see that for an original parameter value  $p_o = 0.2$ :  $\text{OOMPA}(0.2, n_{\text{OOM}} = 1) = 0.1$ ,  $\text{OOMPA}(0.2, n_{\text{OOM}} = 2) = 1.0$  and  $\text{OOMPA}(0.2, n_{\text{OOM}} = 0.5) = 10^{-0.5} \simeq .3162$ .

For simulations with randomized parameters, parameter values were generated from a  $\log_{10}$ -normal distribution [similar to Sobie (2009)] using the equation:

$$p_{\text{rand}} = p_o \cdot 10^{\text{CV} \cdot \text{randn}} \quad (2)$$

where  $p_o$  and  $p_{\text{rand}}$  are the original and randomized parameter value vectors, respectively, and  $\text{randn}$  is a vector with elements sampled from a normal distribution of mean zero and SD 1. CV is a coefficient of variation that quantifies the overall magnitude of the parameter change applied by the OOMPA approximation, calculated by:

$$\text{CV} = \text{stdev}(\log_{10}(p_{\text{OOMPA}}) - \log_{10}(p_o)) \quad (3)$$

Pearson product-moment correlation coefficients (Rodgers and Nicewander, 1988) were computed to compare individual sensitivity coefficients from the original model with perturbed models (using either order-of-magnitude parameter approximations or randomized parameters).

## 3 RESULTS

### 3.1 Order-of-magnitude model of the $\beta$ -adrenergic signaling network

The  $\beta$ -adrenergic signaling network regulates contractility, metabolism and gene expression in the heart (Saucerman and McCulloch, 2006). Ligands (e.g. norepinephrine or isoproterenol) bind to  $\beta_1$ -adrenergic receptors and initiate a series of signaling

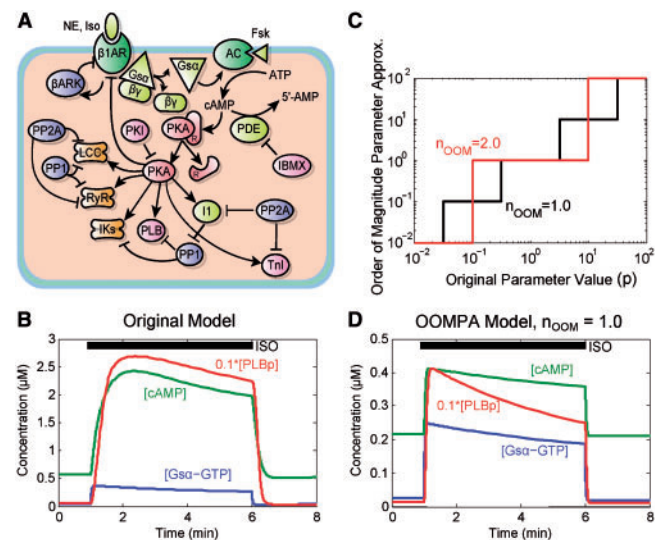


**Fig. 1.** Application of order-of-magnitude parameter approximations to  $\beta$ -adrenergic signaling. (A) Schematic of  $\beta$ -adrenergic signaling model topology. (B) In response to a transient ligand exposure (10 nM ISO), the signaling model predicts time courses for G protein ( $G\alpha$ -GTP) and cyclic AMP (cAMP) activation as well as phospholamban phosphorylation (PLBp). (C) Order-of-magnitude parameter approximations round each model parameter to its nearest whole/fractional order of magnitude. The roughness of each parameter approximation is determined by  $n_{\text{OOM}}$ , where  $n_{\text{OOM}} = 1$  rounds parameters to their nearest one order of magnitude. (D) Time course of model using approximate parameter values ( $n_{\text{OOM}} = 1$ ) in response to transient 10 nM ISO.

events leading to protein kinase A (PKA) activation and substrate phosphorylation (Fig. 1A). The mechanisms of this signaling network were modeled previously using systems of algebraic and ODEs, constrained using biochemical parameters from the experimental literature (Saucerman *et al.*, 2004). The current model uses 86 parameters to predict 23 relevant outputs (state variables). Figure 1B shows example model time course predictions in response to a transient isoproterenol (ISO) exposure. With ISO, G-proteins readily activate ( $G\alpha$ -GTP) and signal to adenylyl cyclase (AC), catalyzing the formation of cyclic AMP (cAMP); cAMP activates PKA, which phosphorylates a number of downstream targets [including phospholamban (PLB)], contributing to the enhanced contractile activity seen in ISO-stimulated cardiac myocytes (Harding *et al.*, 1988).

Construction and parameterization of the  $\beta$ -adrenergic network model greatly benefited from a wealth of prior experimental data. However, such data may not be available for newly discovered or less characterized pathways. Motivated by this challenge, we asked: are this network's core functional properties sensitive to precise biochemical parameter values? To address this question, we applied a mathematical procedure that generated order-of-magnitude parameter approximations (OOMPA) for all model parameters [see Section 2.3, Equation (1)]. This procedure takes an original parameter value  $p$  and rounds it to its nearest order of magnitude; the 'roughness' of the approximation is dictated by the term  $n_{\text{OOM}}$ . For  $n_{\text{OOM}} = 1$ , OOMPA rounds each given parameter to its nearest one order-of-magnitude.  $n_{\text{OOM}} = 2$  will round values to their nearest two orders of magnitude, and so on.

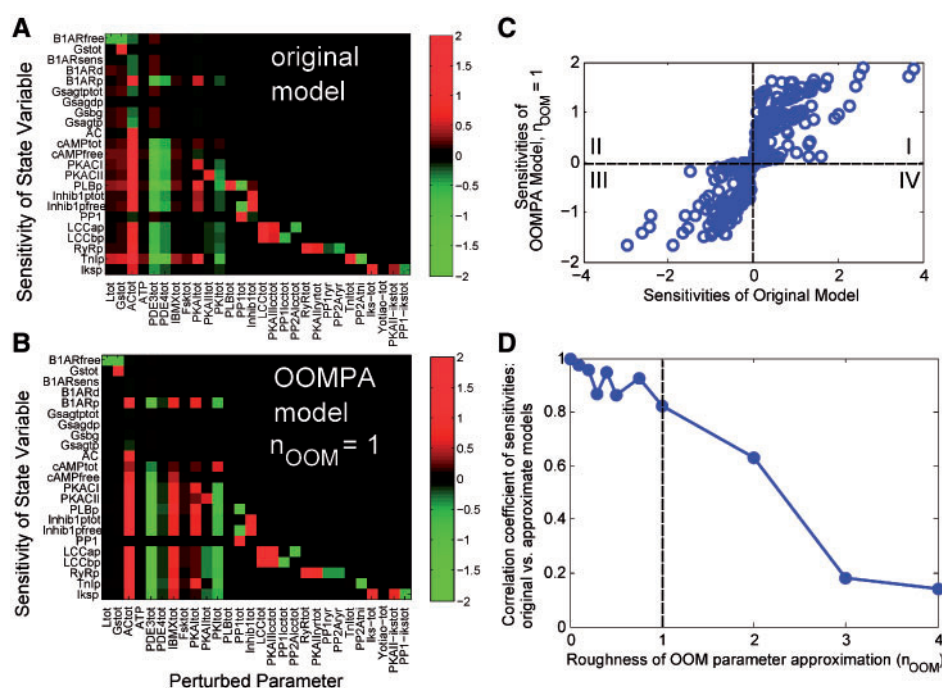


**Fig. 2.** Robustness portrait of  $\beta$ -adrenergic signaling preserved despite order-of-magnitude parameter approximation. (A) Partial sensitivity matrix of original  $\beta$ -adrenergic model, with species ordered upstream to downstream in the pathway. For each ‘experiment’ (column of the matrix), the indicated parameter was increased (5%) from its original value and the resulting steady-state changes in all outputs (state variables) were used to compute individual sensitivity coefficients (rows of the matrix). Thus, the matrix provides a global portrait of the robust and fragile functional relationships in the network. (B) Sensitivity analysis of the order-of-magnitude approximate  $\beta$ -adrenergic model ( $n_{OOM} = 1$ ). (C) Scatter plot of all individual sensitivities from original model (x-axis) and approximate model (y-axis,  $n_{OOM} = 1$ ). A Pearson’s correlation coefficient of 0.82 was computed between these two models, indicating substantial agreement between the two models. (D) Correlation of robustness portraits between original and order-of-magnitude  $\beta$ -adrenergic models with increasing roughness of parameter approximation ( $n_{OOM}$ ). Model performance dropped dramatically at  $n_{OOM} > 2$ , indicating the required parameter precision for proper functionality of this network.

A visualization of the procedure is provided in Figure 1C. Note that larger values of  $n_{OOM}$  restrict parameters to fewer absolute values (e.g.  $n_{OOM} = 2$  restricts parameters to only three values over the depicted range). Figure 1D shows example time courses from an order-of-magnitude  $\beta$ -adrenergic model simulation ( $n_{OOM} = 1$ ) with 10 nM ISO stimulation as in Figure 1B. While quantitative discrepancies are apparent when comparing Figure 1B and D, the kinetics of the original and OOMPA models were qualitatively similar, suggesting preserved core network functionality.

### 3.2 Influence of order-of-magnitude parameter approximations on the robustness portrait of $\beta$ -adrenergic signaling

Previous analysis of this model focused on a few key aspects of  $\beta$ -adrenergic signaling. Here, we sought to more comprehensively investigate this network’s functional relationships. To do this, we systematically perturbed each individual biochemical parameter and plotted the sensitivities of all model outputs as a 2D matrix of sensitivity coefficients (see Section 2.2), obtaining a robustness portrait (Fig. 2A). Given a parameter perturbation  $\Delta P$ , individual sensitivity coefficients were calculated according to  $S_{ij} = (\Delta Y_i / \Delta P_j) (P_{o,j} / Y_{o,i})$ , where  $S_{ij}$  is the steady-state sensitivity of output  $Y_i$  to parameter perturbation  $\Delta P_j$ . State variables are ordered from upstream (receptor level) to downstream (PKA targets) down

the rows of the matrix. Note that the matrix shown in Figure 2A is a reduced version that focuses only on perturbations of total species concentrations (28 of the 86 total parameters). Complete sensitivity matrices are provided in Supplementary Figure S1. In this particular example, parameters were increased 5% from their baseline values (for matrices with varying  $\Delta P$ , see Supplementary Fig. S2). For each ‘perturbation experiment’ (column of the matrix), the model was run to steady state with the indicated parameter perturbation and all model outputs (rows) were compared to their steady-state values from an unperturbed simulation. In all simulations, ligand concentration ( $L_{tot}$ ) was set at a non-saturating dose of 10 nM to allow for detectable changes in outputs (for matrices with varying initial  $L_{tot}$ , see Supplementary Fig. S3).

This analysis highlights several key properties of the  $\beta$ -adrenergic signaling network. Note that the robustness portrait is enriched with a large number of sensitive outputs on its left half, suggesting the network is globally most sensitive to perturbations of upstream components. This result is a function of the network’s topology, where upstream species dictate the level of PKA activation, the main hub in this system. Also, the robustness portrait highlights the role of the negative feedback loop from PKA to the  $\beta_1$  receptor on both upstream and downstream activity levels (PKAI<sub>tot</sub> and PKAI<sub>tot</sub> columns). In addition to these qualitative observations, this analysis allows for quantitative assessment of the network’s most sensitive interactions. Note that a 5% perturbation to the amount of present



ligand (Ltot) results in slight steady-state changes, while the same size perturbation to total [AC] (ACtot) produces larger individual sensitivity coefficients for the same outputs. The network is also very sensitive to the levels of phosphodiesterases (PDEs), which appear to be important negative regulators of this cascade's functionality. Thus, sensitivity analysis of this form provides a unique platform from which the robustness portrait of a signaling network can be explored.

To examine how the precision of biochemical parameters affects the system's robustness portrait, we performed sensitivity analysis on the order-of-magnitude model (Fig. 2B) and compared the results to those of the original model (Fig. 2C). By inspection, global patterns of sensitivities are well preserved by the approximate model. Note that both models are highly sensitive to perturbations of certain species (e.g. AC and PDEs) but less so for others (e.g. PKA substrates LCC and RyR). A Pearson's correlation coefficient of 0.82 was computed between the individual sensitivities of the two models, indicating substantial quantitative agreement. In addition, all sensitivities were in the 1st or 3rd quadrants of Figure 2C, indicating no major qualitative discrepancies. While the focus here is a systematic comparison to the original validated biochemical model, the predictions of the order-of-magnitude  $\beta$ -adrenergic model are also consistent with a wide range of published experimental measurements on this pathway (Supplementary Table S1). Thus, this network's steady-state properties appear to be robust to the precision of biochemical parameters within an order of magnitude.

Given that predictions from the approximate model with  $n_{\text{OOM}} = 1$  were quite similar to the original model, we compared additional approximate models of varying  $n_{\text{OOM}}$  (0.1–4) to determine how fine-tuned the biochemical parameters must be to obtain accurate predictions of functional relationships. For the  $\beta$ -adrenergic network, even rounding biochemical parameters to the nearest two orders of magnitude ( $n_{\text{OOM}}=2$ ) still produced reasonably informative predictions ( $r=0.63$ ), but models with  $n_{\text{OOM}} > 2$  performed poorly ( $r < 0.2$ ) (Fig. 2D; see Supplementary Fig. S4 for original sensitivity matrices). Thus, the steady-state behavior of the  $\beta$ -adrenergic network is remarkably robust to the precise values of its biochemical parameters, but knowledge of network topology alone is insufficient for accurate predictions. In contrast, the kinetic time courses of the 23 species (shown partially in Fig. 1D) were more sensitive to parameter precision, yielding a moderate Pearson's correlation coefficient of 0.32.

### 3.3 Order-of-magnitude approximations outperform randomized models

The above analysis indicates that the steady-state functional properties of  $\beta$ -adrenergic signaling were preserved when parameters were approximated to their nearest two orders of magnitude. Given these observations, we next asked whether or not similar results are obtained when parameter values are assigned at random. To address this question, we ran additional simulations in which all model parameters were simultaneously perturbed by random noise. Individual parameter noise strengths were randomly drawn from  $\log_{10}$ -normal distributions whose variances were equivalent to those of order-of-magnitude models (see Section 2). For example,  $n_{\text{OOM}} = 1$  (rounding to the nearest 1 order of magnitude) had a coefficient of variation (CV) of 0.2991;

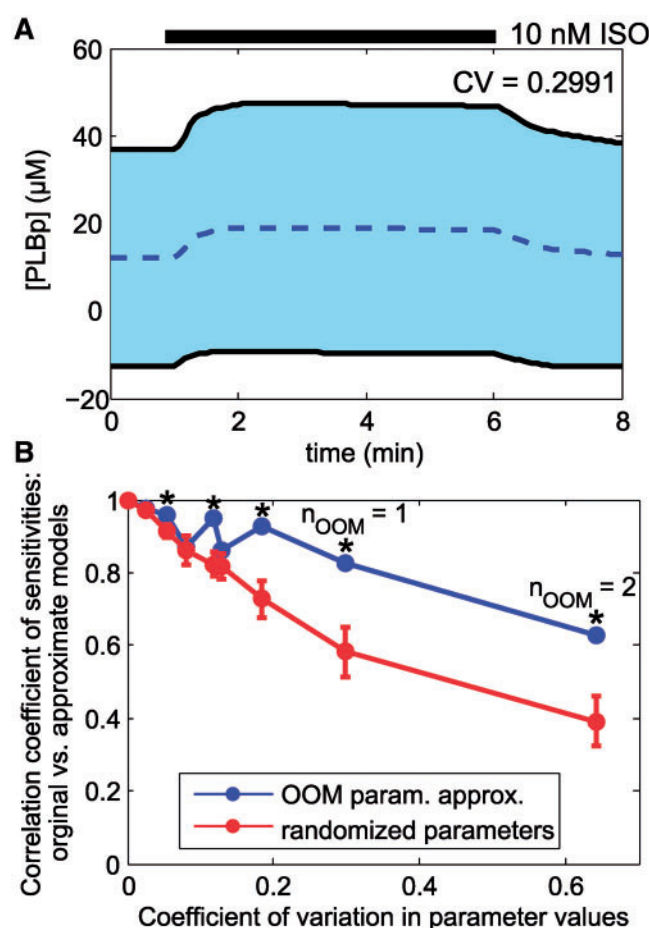


**Fig. 3.** Order-of-magnitude model predictions outperform those of randomized models with equivalent parameter variance. (A) Average phospholamban phosphorylation (PLBp) (dashed line) and confidence interval (shaded area,  $\pm 1$  SD) computed from 100 randomized model runs ( $CV=0.2991$ ). (B) Pearson's correlation coefficients were computed between the individual sensitivities of randomized models with increasing parameter variance and those of the original model (red line). These results are compared to order-of-magnitude models (blue line) of equivalent parameter variance, as determined by the change from their original values [see Equation (3)]. Asterisk represents statistical significance of the randomized models compared with order-of-magnitude models assessed at  $P < 0.001$  by one-sample  $t$ -test with Bonferroni correction for multiple comparisons. Error bars are 95% confidence intervals for the mean.

this value was used as the variance for parameter noise when comparing randomized models to  $n_{\text{OOM}} = 1$  models. More than 50 randomized simulations were run for each CV tested.

The effects of parameter randomization on PLB phosphorylation dynamics for  $CV = 0.2991$  (equivalent to the parameter changes with  $n_{\text{OOM}} = 1$ ) are shown in Figure 3A. With parameter randomization, predicted kinetics can differ considerably from the original model, similar to the kinetic results from order-of-magnitude models. But are steady-state network properties similarly preserved in response to random parameter fluctuations? We found that the robustness portraits of order-of-magnitude models were statistically more strongly correlated with the original model than were those of the randomized models, especially as CV increased

**Table 1.** List of 10 additional biological networks analyzed

Name	Model description	No. of Variables	No. of Parameters	References
<i>Escherichia coli</i> chemotaxis	Tar receptor signaling to CheW and CheA	22	47	Bray and Bourret (1995)
EGF	EGF receptor and downstream Ras/Erk signaling	93	91	Schoeberl <i>et al.</i> (2002)
MAPK	Scaffold proteins regulating the MAPK pathway	86	300	Levchenko <i>et al.</i> (2000)
Stem cell	Oct4/Sox2/Nanog transcriptional network for stem cell differentiation	8	49	Chickarmane and Peterson (2008)
CaMKII	CaMKII and calcineurin signaling in neurons	44	82	Bhalla (2004)
Apoptosis	TRAIL and caspase signaling in apoptosis	58	71	Albeck <i>et al.</i> (2008)
IL6	IL6, JAK/STAT signaling in hepatocytes	66	107	Singh <i>et al.</i> (2006)
Lac operon	Feedback regulation of the lactose operon in <i>E.coli</i>	8	24	Yildirim and Mackey, (2003)
Wnt, Erk	Positive feedback and crosstalk between Wnt and Erk, involved in carcinogenesis	28	59	Kim <i>et al.</i> (2007)
NFκB	NFκB/IκB module and dynamics	24	37	Hoffmann <i>et al.</i> (2002)

(Fig. 3B). For example, at  $CV=0.2991$ , randomized  $\beta$ -adrenergic models had an average correlation coefficient of just 0.58 compared with the original  $\beta$ -adrenergic model. Order-of-magnitude models outperformed randomized models, because all order-of-magnitude parameter perturbations were generally restricted to that particular order-of-magnitude, while randomized perturbations could occasionally be larger.

### 3.4 Application of order-of-magnitude approximation to 10 additional biological networks

The above results indicate that the steady-state properties of the cardiac  $\beta$ -adrenergic signaling network are robust to order-of-magnitude parameter approximations within two orders of magnitude. We next asked whether this robustness property may be generalized to other biological networks. We extended this analysis to 10 additional computational models, 9 of which are curated models from the BioModels database (Le Novère *et al.*, 2006) and 1 (Bhalla, 2004) from the DOQCS (Sivakumaran *et al.*, 2003) (Table 1). These specific models were chosen in an attempt to survey a wide range of biological networks of varying size and function. As done with the  $\beta$ -adrenergic signaling network, we generated order-of-magnitude parameter approximations for each model ( $n_{OOM}=0.1, 0.5, 1, 2, 3$  and 4), performed sensitivity analysis on each model and computed correlation coefficients between the robustness portrait of each approximate model and its corresponding original model's robustness portrait (Fig. 4 and Supplementary Fig. S5). Note that  $n_{OOM}=0$  in Figure 4 indicates comparisons

between each default model and itself, which produces  $r=1$  in all cases.

In general, order-of-magnitude models with  $n_{OOM} \leq 1$  strongly correlated with their corresponding default models. Nine out of ten networks produced correlation coefficients  $>0.75$  for  $n_{OOM}=1$ , though correlation typically dropped dramatically when  $n_{OOM} \geq 3$ . Given that one model, the lac operon gene circuit (Yildirim and Mackey, 2003), performed quite poorly at  $n_{OOM} \geq 1$ , we investigated whether there were certain network features that could explain its weaker overall performance. We first hypothesized that network size could be an important predictive feature for robustness to order-of-magnitude parameter precision. However, we observed a weak relationship between model size and network robustness: correlation coefficients at  $n_{OOM}=1$  for all tested models only weakly correlated with model size in terms of number of state variables ( $r=0.41$ ) or number of parameters ( $r=0.19$ ) (Supplementary Fig. S4). Another explanation could be the existence of multistable states, whereby slight parameter adjustments allow networks to traverse a bifurcation. Bifurcations, by definition, alter the qualitative behavior of a system as a result of small changes in its underlying parameters (Strogatz, 1994). Indeed, the lac operon network model contains a bifurcation (Yildirim and Mackey, 2003), which contributed to its poor overall performance during our analysis. But not all such models perform poorly: the CaMKII and stem cell models also exhibit multistability, yet are globally much more robust to order-of-magnitude approximation. Thus, the observation of conserved robustness portraits despite order-of-magnitude parameter uncertainty applies to a wide range of biological networks.

## 4 DISCUSSION

In this study, we computationally explored conservation of global functional relationships in biological signaling networks in the face parameter imprecision. Starting with a biochemically detailed computational model of cardiac  $\beta$ -adrenergic signaling (Saucerman *et al.*, 2004), order-of-magnitude analysis revealed that this network shows a steady-state 'robustness portrait' that is insensitive to parameter precision within two orders of magnitude. However, predictive capability was lost when parameter approximations became very rough ( $n_{OOM} \geq 3$ ) or when parameters were randomly assigned, suggesting that this network's function depends on both network topology and biochemical parameter precision within 1–2 orders of magnitude. We then extended this analysis to 10 additional signaling networks, finding that key properties of these networks were also generally preserved when order-of-magnitude approximations were applied. Thus, the steady-state robustness portrait of a signaling network can be predicted even when parameter data are imprecise. This systems insight suggests a rational approach for prioritizing experiments toward the most fragile elements of a network, driving subsequent model revision and quantitative understanding.

### 4.1 Sensitivity and order-of-magnitude analysis of cardiac $\beta$ -adrenergic signaling

The  $\beta$ -adrenergic signaling network is a key regulator of contractility, metabolism and gene expression in the heart (Saucerman and McCulloch, 2006). Prior computational modeling

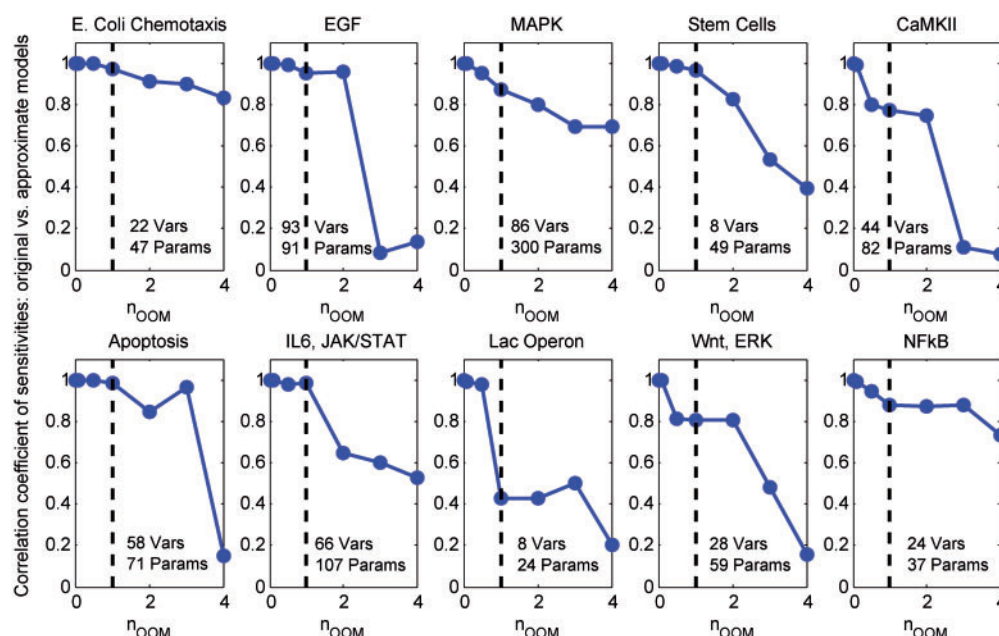


**Fig. 4.** Order-of-magnitude parameter approximations retain core functional properties of 10 diverse biological networks. Models of 10 diverse biological systems were obtained from the BioModels or DOQCS databases (listed in Table 1). Order-of-magnitude approximations were applied to each model with varying  $n_{OOM}$  (0.1, 0.5, 1, 2, 3 and 4) and correlations between approximate and original model sensitivities were computed. At  $n_{OOM} = 1$ , Pearson's correlation coefficients were  $>0.75$  for 9 out of 10 models. Beyond two orders of magnitude, predictive power typically dropped dramatically.

of the  $\beta$ -adrenergic signaling network has revealed a number of new specific insights into its function (Saucerman *et al.*, 2003, 2004), but this study provided a more comprehensive view of how each of the network's components affect each other in the network. We found that this network is globally differentially sensitive to equivalent quantitative perturbations in some species (e.g. total [AC] and [PDE]) as opposed to others (e.g. small changes in ligand). Such information was not readily apparent from our previous analyses, but is consistent with experimental data (Supplementary Table S1).

Development of the original  $\beta$ -adrenergic model was largely facilitated by a wealth of prior experimental work that aided model parameterization. Given that such data may not be readily available for newly discovered pathways, we were motivated to assess the importance of using tightly constrained parameter values in this model system. We used order-of-magnitude approximations to determine whether or not rough estimates of biochemical parameter values would still capture the global functional properties of this network. Order-of-magnitude approximations are widely used in engineering and physics, and their use here demonstrates utility for analysis of complex biological networks. Original and approximate models were compared based on their robustness portraits rather than the magnitude of state variables, because identifying sensitive components is typically more important for prioritizing experimental studies.

Order-of-magnitude analysis revealed that steady-state functional relationships in this network are quite robust to the precision of parameter values, while signaling kinetics are more sensitive. This finding is consistent with prior analyses of other systems. In bacterial chemotaxis, steady-state adaptation is remarkably robust, though the kinetics of adaptation vary considerably when parameters fluctuate

(Barkai and Leibler, 1997). In the EGF signaling network, accurate prediction of kinetics required extremely precise direct parameter measurements, although steady-state functional relationships were not examined (Gutenkunst *et al.*, 2007). Interestingly, the same study showed that the kinetics of EGF and many other signaling pathways could be numerically fit to data by many distinct parameter combinations due to the high degree of parameter covariance or 'sloppiness' (Gutenkunst *et al.*, 2007).

## 4.2 Generality of results and implications for future work

To determine the generality of the results obtained from our analysis of  $\beta$ -adrenergic signaling, we applied order-of-magnitude approximation to 10 additional biological networks. The steady-state robustness portraits for most of these networks were also conserved for parameter values within one or two orders of magnitude. This suggests that the conclusions regarding order-of-magnitude parameter sensitivities in  $\beta$ -adrenergic signaling are applicable across a wide range of biological processes. However, we did encounter one network where parameter approximation more substantially affected its robustness portrait. In particular, the lac operon model contained a bifurcation that qualitatively affected the functionality of the network at  $n_{OOM} = 1$ . This represents a specific case where the underlying network parameters exert a major influence over a network's core functionality. While robustness of the mono- and multi-stable systems examined here focused on the steady state, this analysis could be extended to quantify dynamic features such as decay rates or the period and phase properties of oscillations as performed for circadian rhythms (Bagheri *et al.*, 2007).



The results shown here are consistent with previous studies of network robustness to parameter variation. Von Dassow *et al.* examined the segment polarity genetic network in *Drosophila* and, using Monte Carlo sampling of the parameter space, showed that a wide range of parameter combinations could predict the desired developmental patterning (von Dassow *et al.*, 2000). The geometry of parameter space for this segment polarity network was subsequently examined further, finding that on average the phenotype was maintained during a random walk in parameter space for ~2000 steps (Dayarian *et al.*, 2009). Rather than taking random walks in parameter space, in the current study we identified an efficient deterministic approach to quantify the necessary parameter precision in experimentally relevant units (e.g. 1 order-of-magnitude). With our analysis, we examined the effects of parameter precision on the robustness portrait, a global quantitative measure of functional relationships between all network species, rather than focusing on a single, qualitative phenotype. Further, this analysis was performed on 11 biological networks, demonstrating remarkable similarity across biological systems. Benetele *et al.* developed a model of apoptosis signaling in which they generated sensitivity matrices similar to those shown here (Bentele *et al.*, 2004). While they also found that most sensitivities were robust to variations in parameter values in their apoptosis model, the degree of parameter precision needed to accurately predict the sensitivity matrix was not quantified. Instead, the focus there was on using sensitivity analysis to systematically reduce model complexity and estimate parameter values (Bentele *et al.*, 2004). Thus, our analysis extends previous concepts of robustness to parameter variation, quantifying how parameter precision affects the global network relationships across a diverse range of biological networks.

Overall, our results indicate that sensitivity analysis can help reveal critical regulatory patterns within a signaling network, even with imprecise parameter values. Not only can this analysis help visualize functional dependencies between network constituents, it can also reveal critical nodes most sensitive to perturbations. Such analysis is useful from a modeling perspective, but can also aid experimentalists by providing a framework from which future experiments can be prioritized. As an example, we found that the  $\beta$ -adrenergic signaling network was very sensitive to active levels of PDEs. Notably, PDE inhibition is an active area of research for the treatment of chronic heart failure (Van Tassell *et al.*, 2008). Such unification of computational and experimental studies can facilitate more comprehensive understanding of global network functionality and aid in the search for new therapeutic avenues to complex diseases.

**Funding:** National Institutes of Health (HL094476 to J.J.S.); American Heart Association (0830470N to J.J.S.).

**Conflicts of interest:** none declared.

## REFERENCES

Albeck,J.G. *et al.* (2008) Quantitative analysis of pathways controlling extrinsic apoptosis in single cells. *Mol. Cell*, **30**, 11–25.  
 Alon,U. *et al.* (1999) Robustness in bacterial chemotaxis. *Nature*, **397**, 168–171.  
 Bagheri,N. *et al.* (2007) Quantitative performance metrics for robustness in circadian rhythms. *Bioinformatics*, **23**, 358–364.  
 Barkai,N. and Leibler,S. (1997) Robustness in simple biochemical networks. *Nature*, **387**, 913–917.  
 Bentele,M. *et al.* (2004) Mathematical modeling reveals threshold mechanism in CD95-induced apoptosis. *J. Cell Biol.*, **166**, 839–851.

Bhalla,U.S. (2004) Signaling in small subcellular volumes. I. Stochastic and diffusion effects on individual pathways. *Biophys. J.*, **87**, 733–744.  
 Bray,D. and Bourret,R.B. (1995) Computer analysis of the binding reactions leading to a transmembrane receptor-linked multiprotein complex involved in bacterial chemotaxis. *Mol. Biol. Cell*, **6**, 1367–1380.  
 Chickarmane,V. and Peterson,C. (2008) A computational model for understanding stem cell, trophectoderm and endoderm lineage determination. *PLoS One*, **3**, e3478.  
 Csete,M.E. and Doyle,J.C. (2002) Reverse engineering of biological complexity. *Science*, **295**, 1664–1669.  
 Dayarian,A. *et al.* (2009) Shape, size, and robustness: feasible regions in the parameter space of biochemical networks. *PLoS Comput. Biol.*, **5**, e1000256.  
 Gutenkunst,R.N. *et al.* (2007) Universally sloppy parameter sensitivities in systems biology models. *PLoS Comput. Biol.*, **3**, 1871–1878.  
 Harding,S.E. *et al.* (1988) Contractile responses of isolated adult rat and rabbit cardiac myocytes to isoproterenol and calcium. *J. Mol. Cell. Cardiol.*, **20**, 635–647.  
 Hoffmann,A. *et al.* (2002) The IkappaB-NF-kappaB signaling module: temporal control and selective gene activation. *Science*, **298**, 1241–1245.  
 Kim,D. *et al.* (2007) A hidden oncogenic positive feedback loop caused by crosstalk between Wnt and ERK pathways. *Oncogene*, **26**, 4571–4579.  
 Kitano,H. (2004) Biological robustness. *Nat. Rev.*, **5**, 826–837.  
 Kollmann,M. *et al.* (2005) Design principles of a bacterial signalling network. *Nature*, **438**, 504–507.  
 Krantz,M. *et al.* (2009) Robustness and fragility in the yeast high osmolarity glycerol (HOG) signal-transduction pathway. *Mol. Syst. Biol.*, **5**, 281.  
 Le Novère,N. *et al.* (2006) BioModels Database: a free, centralized database of curated, published, quantitative kinetic models of biochemical and cellular systems. *Nucleic Acids Res.*, **34**, D689–691.  
 Levchenko,A. *et al.* (2000) Scaffold proteins may biphasically affect the levels of mitogen-activated protein kinase signaling and reduce its threshold properties. *Proc. Natl Acad. Sci. USA*, **97**, 5818–5823.  
 Meir,E. *et al.* (2002) Robustness, flexibility, and the role of lateral inhibition in the neurogenic network *Curr. Biol.*, **12**, 778–786.  
 Muzzey,D. *et al.* (2009) A systems-level analysis of perfect adaptation in yeast osmoregulation. *Cell*, **138**, 160–171.  
 Paszek,P. *et al.* (2010) Population robustness arising from cellular heterogeneity. *Proc. Natl Acad. Sci. USA*, **107**, 11644–11649.  
 Rodgers,J.L. and Nicewander,W.A. (1988) 13 ways to look at the correlation-coefficient. *Am. Stat.*, **42**, 59–66.  
 Saucerman,J.J. and McCulloch,A.D. (2006) Cardiac beta-adrenergic signaling: from subcellular microdomains to heart failure. *Ann. N Y Acad. Sci.*, **1080**, 348–361.  
 Saucerman,J.J. *et al.* (2003) Modeling beta-adrenergic control of cardiac myocyte contractility in silico. *J. Biol. Chem.*, **278**, 47997–48003.  
 Saucerman,J.J. *et al.* (2004) Proarrhythmic consequences of a KCNQ1 AKAP-binding domain mutation: computational models of whole cells and heterogeneous tissue. *Circ. Res.*, **95**, 1216–1224.  
 Sauro,H.M. *et al.* (2003) Next generation simulation tools: the systems biology workbench and BioSPICE integration. *Omics*, **7**, 355–372.  
 Schoeberl,B. *et al.* (2002) Computational modeling of the dynamics of the MAP kinase cascade activated by surface and internalized EGF receptors. *Nat. Biotechnol.*, **20**, 370–375.  
 Shinar,G. and Feinberg,M. (2010) Structural sources of robustness in biochemical reaction networks. *Science*, **327**, 1389–1391.  
 Singh,A. *et al.* (2006) Modeling regulatory mechanisms in IL-6 signal transduction in hepatocytes. *Biotechnol. Bioeng.*, **95**, 850–862.  
 Sivakumaran,S. *et al.* (2003) The database of quantitative cellular signaling: management and analysis of chemical kinetic models of signaling networks. *Bioinformatics*, **19**, 408–415.  
 Sobie,E.A. (2009) Parameter sensitivity analysis in electrophysiological models using multivariable regression. *Biophys. J.*, **96**, 1264–1274.  
 Stelling,J. *et al.* (2004) Robustness of cellular functions. *Cell*, **118**, 675–685.  
 Strogatz,S.H. (1994) *Nonlinear Dynamics and Chaos : with Applications to Physics, Biology, Chemistry, and Engineering*. Addison-Wesley Pub., Reading, MA.  
 Tay,S. *et al.* (2010) Single-cell NF-kappaB dynamics reveal digital activation and analogue information processing. *Nature*, **466**, 267–271.  
 Van Tassell,B.W. *et al.* (2008) Combination therapy with beta-adrenergic receptor antagonists and phosphodiesterase inhibitors for chronic heart failure. *Pharmacotherapy*, **28**, 1523–1530.  
 von Dassow,G. *et al.* (2000) The segment polarity network is a robust developmental module. *Nature*, **406**, 188–192.  
 Yildirim,N. and Mackey,M.C. (2003) Feedback regulation in the lactose operon: a mathematical modeling study and comparison with experimental data. *Biophys. J.*, **84**, 2841–2851.